Conservative and disruptive modes of adolescent change in human brain functional connectivity

František Váša[a,b,1], Rafael Romero-Garcia[a], Manfred G. Kitzbichler[a], Jakob Seidlitz[a,c], Kirstie J. Whitaker[a,d], Matilde M. Vaghi[e,h], Prantik Kundu[f], Ameera X. Patel[a], Peter Fonagy[g], Raymond J. Dolan[e,h], Peter B. Jones[a,j], Ian M. Goodyer[a], the NSPN Consortium[‡a], Petra E. Vértes[a,d,i,2], and Edward T. Bullmore[a,j,2]

[a]Department of Psychiatry, University of Cambridge, Cambridge, CB2 0SZ, UK; [b]Department of Neuroimaging, Institute of Psychiatry, Psychology and Neurosciences, King's College London, London, SE5 8AF, UK; [c]Developmental Neurogenomics Unit, National Institute of Mental Health, Bethesda, MD 20892, USA; [d]The Alan Turing Institute, London, NW1 2DB, UK; [e]Wellcome Trust Centre for Neuroimaging, UCL Institute of Neurology, University College London, London WC1N 3BG, UK; [f]Brain Imaging Center, Icahn School of Medicine at Mount Sinai, New York, NY 10029, USA; [g]Research Department of Clinical, Educational and Health Psychology, University College London, London WC1E 6BT, UK; [h]Max Planck UCL Centre for Computational Psychiatry and Ageing Research, University College London, London WC1B 5EH, UK; [i]School of Mathematical Sciences, Queen Mary University of London, London E1 4NS, UK; [j]Cambridgeshire and Peterborough NHS Foundation Trust, Huntingdon, PE29 3RJ, UK

This manuscript was compiled on November 19, 2019

Adolescent changes in human brain function are not entirely understood. Here we used multi-echo functional magnetic resonance imaging (fMRI) to measure developmental change in functional connectivity (FC) of resting-state oscillations between pairs of 330 cortical regions and 16 subcortical regions in 298 healthy adolescents scanned 520 times. Participants were aged 14-26 years, and were scanned on one to three occasions at least 6 months apart. We found two distinct modes of age-related change in FC: "conservative" and "disruptive". Conservative development was characteristic of primary cortex, which was strongly connected at 14 years and became even more connected in the period 14-26 years. Disruptive development was characteristic of association cortex and subcortical regions, where connectivity was re-modelled: connections that were weak at 14 years became stronger during adolescence, and connections that were strong at 14 years became weaker. These modes of development were quantified using the maturational index (MI), estimated as Spearman's correlation between edge-wise baseline FC (at 14 years, FC_{14}) and adolescent change in FC (ΔFC_{14-26}), at each region. Disruptive systems (with negative MI) were activated by social cognition and autobiographical memory tasks in prior fMRI data, and significantly co-located with prior maps of aerobic glycolysis (AG), AG-related gene expression, post-natal cortical surface expansion, and adolescent shrinkage of cortical thickness. The presence of these two modes of development was robust to numerous sensitivity analyses. We conclude that human brain organisation is disrupted during adolescence by re-modeling of functional connectivity between association cortical and subcortical areas.

neurodevelopment | connectome | MRI | Allen Human Brain Atlas | head movement

During adolescence the human brain undergoes substantial changes in both structure (1, 2) and function (3, 4). Accurately describing these maturational processes is key to understanding the parallel changes in cognition and behaviour, as well as the vulnerability to mental health disorders (5), that characterize this critical developmental period.

Functional brain networks derived from fMRI have proven to be useful for understanding large-scale brain organization (6, 7). The nodes of these fMRI networks correspond to macroscopic brain regions and the edges correspond to the correlations in brain activity, or so-called functional connectivity (FC), between pairs of regionally localised, low frequency oscillations. Several studies have reported age-related changes in functional brain networks during adolescence, but the findings are overall somewhat inconsistent. This is likely due in part to small sample sizes, the lack of longitudinal data, and significant variation in fMRI data pre-processing and analysis methods (see SI Appendix, Table S1). In addition, although subcortical nuclei are theoretically well-recognised components of frontal cortico-striato-thalamic circuits, subcortical connectivity has generally been measured only for a few nuclei or ignored altogether (see SI Appendix, Table S2).

Multiple prior resting-state fMRI studies of human brain development in childhood and adolescence replicably reported an age-related increase in the strength of long-range connections accompanied by a decrease in the strength of short-range connections (8–11). Since long-range connections tend to be concentrated on association cortical areas involved in higher-order cognitive functions, these results were consistent with prior work suggesting that primary sensory and motor areas mature earlier in childhood, whereas association areas show relatively protracted maturation, extending into adolescence and early adulthood (1, 2, 12–14).

However, it has since become clear that these changes in FC attributed to age might have been confounded by the effects of in-scanner head motion (13, 15–17). It is now well-

Significance Statement

How does the human brain change during adolescence? We found two distinct modes of change in functional connectivity between brain regions, "conservative" and "disruptive", measured using fMRI in healthy young people (14-26 years old). Conservative regions, often specialised for basic sensory and motor functions, were strongly connected at age 14, before strengthening more by age 26. Whereas disruptive regions, that were activated by complex tasks like theory-of-mind and autobiographical memory, comprised both connections that were weak at age 14 but strengthened by age 26, and connections that were strong at age 14 but weakened by age 26. Disruptive maturation of fMRI connectivity between cortex and subcortex could represent metabolically costly re-modelling of brain structure that underpins development of adult faculties.

Author contributions: P.F., R.J.D., P.B.J., I.M.G. and E.T.B. designed the NSPN study; F.V, P.E.V., and E.T.B. designed analyses; F.V., R.R.G., M.G.K., J.S., K.J.W., M.M.V. and P.E.V. processed and quality controlled data; J.S., P.K., and A.X.P. contributed new analytic tools; F.V. and P.E.V. analyzed data; and F.V., P.E.V., E.T.B. wrote the paper.

[2] P.E.V. and E.T.B. are joint last authors.

[1]To whom correspondence should be addressed. E-mail: fdv247@gmail.com

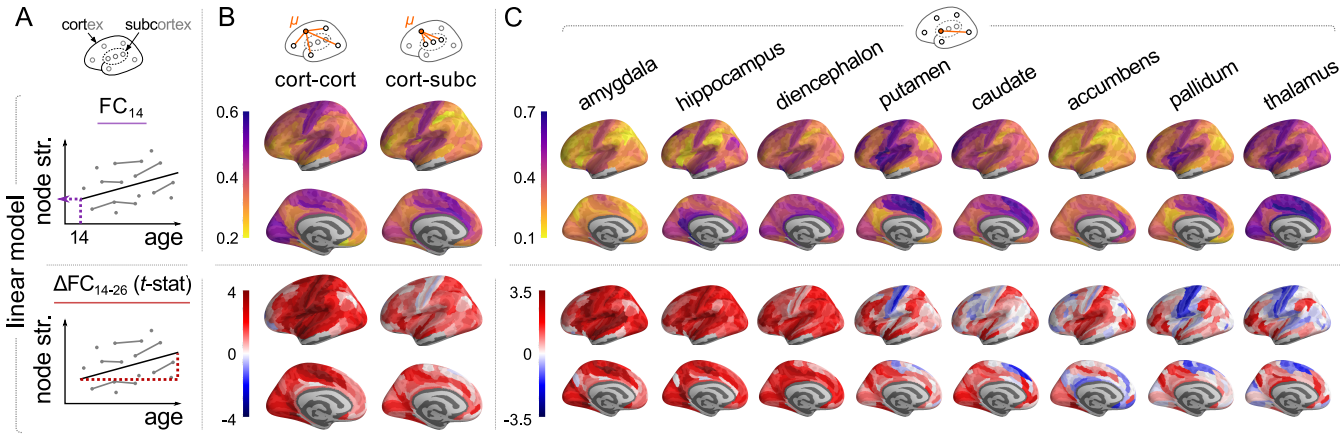

Fig. 1. Regional strength of functional connectivity (weighted degree) of cortical areas and subcortical nuclei at 14 years (FC_{14}) and regional change in strength of connectivity during adolescence (ΔFC_{14-26}). A) Regional strength for each of 330 cortical and 16 subcortical nodes was regressed on a linear function of age for all participants (N = 520 scans from 298 participants; mixed effects model). B) Parameters of cortico-cortical (left) and cortico-subcortical connectivity (connectivity). For subcortico-cortical and subcortico-subcortical connectivity, see SI Appendix, Fig. S4. C) Heterogeneous FC_{14} and ΔFC_{14-26} of individual subcortical nuclei to cortex (subcortical regions are ordered by decreasing average rate of change). Due to bilateral symmetry and space constraints, only left hemispheres are visualised.

recognised that small (<1 mm), transient head movements during scannning can bias estimation of correlations between fMRI time series and this is a critical issue for developmental studies because younger participants may find it more difficult to remain stationary in the scanner.

Here, we measured resting-state FC maturation in an accelerated longitudinal study of 298 healthy adolescents, aged 14-26 years, scanned one to three times. To correct fMRI time series for effects of participant in-scanner motion, we used multi-echo scans (18) denoised using multi-echo independent component analysis (ME-ICA; 19, 20) to identify and discard components of fMRI time series unrelated to the BOLD signal. We further corrected residual effects of head motion using linear regression, and investigated robustness of our findings to head movement by extensive supplementary analyses. For each pre-processed fMRI dataset, we estimated the Pearson's correlation between all pairs of regional mean time series from each of 330 cortical areas and 16 subcortical nuclei. We identified two modes of developmental change in fMRI connectivity, defined by positive or negative maturational index (MI), and assessed the psychological and biological relevance of these so-called "conservative" or "disruptive" systems by meta-analysis of prior task-related fMRI data and by testing for anatomical co-location of the MI map with prior maps of cortical metabolism, gene expression, post-natal areal expansion and adolescent cortical shrinkage.

Results

Head movement. A total of 36 scans were excluded by one or more quality control criteria, including high in-scanner motion (μ(FD) > 0.3 mm or max(FD) > 1.3 mm; see SI Appendix). Following scan exclusion, regional fMRI time series were available at 330 cortical areas and 16 subcortical structures for 298 participants (151 females), scanned a total of 520 times (see SI Appendix text and Fig. S1).

In these data, we found no evidence of an age-related change in head movement, indexed by framewise displacement (FD; 15). However, there was a positive correlation between FC and head movement, and also distance dependence of the correlation between FC and FD, which was greater when the distance between nodes was greater (SI Appendix, Fig. S2). These confounding effects of head movement on connectivity in ME-ICA pre-processed data were corrected by regressing FC on mean FD (21, 22). The residual (mean FD-corrected) estimates of FC were not significantly correlated with head motion and there was no distance dependence of the relationship between residual FC and FD (SI Appendix, Fig. S2). We therefore used this movement correction pipeline of ME-ICA followed by FD regression as the basis for further analysis of functional connectivity. We subsequently confirmed that the results obtained from our main analysis (N = 520) were qualitatively and quantitatively consistent with the results obtained by a sensitivity analysis using only a subset of "low-motion" fMRI data (N = 182) that had been acquired without discernible head motion (FD < 0.2 mm for each of 100 consecutive volumes; 23) and analysed without FD-regression (SI Appendix, Fig. S24-28 and Fig. S36-37). To test robustness of our results to an alternative movement correction strategy, we also used global signal regression (GSR) for movement correction of the whole sample (N = 520) and obtained results that were qualitatively consistent and correlated with results obtained both from our main analysis and the low-motion data (SI Appendix, Fig. S29-35 and Fig. S36-37).

Age-related change of connectivity strength. The functional connectivity (FC), or weight of an edge between two nodes, as defined by the correlation between a pair of regional fMRI time series, was generally positive. The global mean correlation weakly increased with age ($t(221) = 2.3$, $P = 0.023$; SI Appendix, Fig. S3). For each regional node, we estimated its strength of connectivity (or weighted degree) by averaging the correlations between it and all other regions. We also calculated the strength of connectivity specifically within or between cortical and subcortical subsets of nodes. Using a mixed effect linear model of age-related change, we estimated the "baseline" strength of FC at age 14 years, FC_{14}, and the linear rate of change in weighted degree as a function of age, ΔFC_{14-26} (Fig. 1A), for each node. We also estimated the baseline and age-related change in FC for each edge.

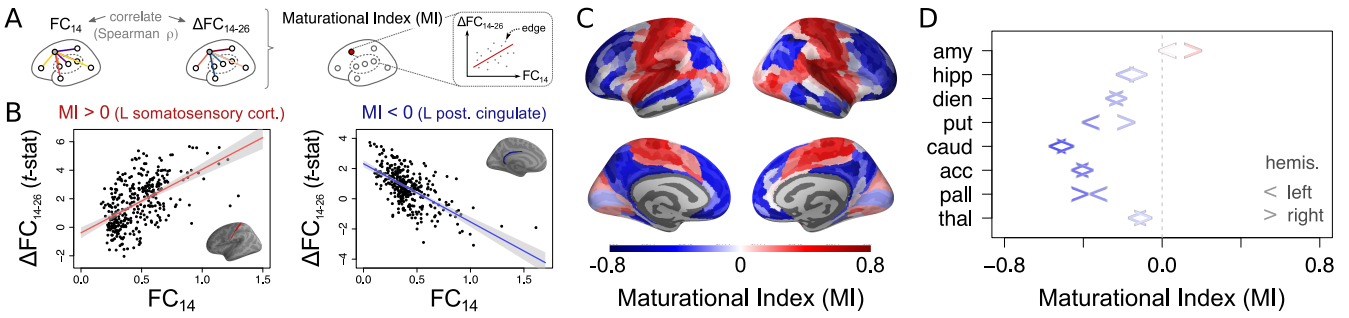

Fig. 2. Maturational index. A) The maturational index (MI) for each brain region is defined as the correlation of edge-wise baseline FC_{14} versus rate of change ΔFC_{14-26}. Panel B) Estimation of MI is illustrated for two exemplar regions: left somatosensory cortex which illustrates a "conservative" mode of development with positive MI; and left posterior cingulate cortex which illustrates a "disruptive" mode of development with negative MI. C) Visualisation of the Maturational Index for all cortical regions, and D) subcortical regions (the left/right arrow corresponds to the left/right hemisphere).

At 14 years, all cortical regions had positive cortico-cortical connectivity strength and the most strongly connected nodes were located in primary motor and sensory cortical areas. Cortico-subcortical connectivity strength had a similar anatomical distribution, with stronger connectivity between primary cortical areas and subcortex, at baseline (Fig. 1B). Age-related rates of change in connectivity strength were also regionally heterogeneous. Cortico-cortical connectivity strength increased in most regions during adolescence, most rapidly in primary motor and sensory cortex. However, age-related change in the strength of cortico-subcortical connectivity had a different anatomical distribution. The most positive rates of increase in connectivity were between subcortical nodes and association cortical areas, whereas some primary motor and sensory cortical areas had negative age-related changes in strength of connectivity with subcortical regions (Fig. 1B).

To further investigate cortico-subcortical connectivity, we estimated FC_{14} and ΔFC_{14-26} between each cortical area and each bilateral pair of 8 subcortical regions (Fig. 1C). At baseline, the putamen, the pallidum and the thalamus were strongly connected to many cortical areas; whereas the amygdala and the accumbens had somewhat lower strength of cortical connectivity overall. Over the course of adolescence, the amygdala ($P_{\mathrm{FDR}} < 0.05$), the hippocampus ($P_{\mathrm{FDR}} < 0.05$) and the diencephalon had increased cortical connectivity; whereas the putamen, the pallidum, and the thalamus, had decreased strength of connectivity with primary somatomotor and premotor cortex, but increased strength of connectivity to frontal and parietal association cortex. See SI Appendix (Fig. S4 and Table S3) for details.

Maturational index. For each regional node, there was often a strong relationship between baseline connectivity FC_{14} and adolescent change in connectivity ΔFC_{14-26} for the 345 edges connecting it to the rest of the network. We defined the maturational index (MI) as the signed coefficient (Spearman's ρ) of the relationship between FC_{14} and ΔFC_{14-26} for each node (Fig. 2A). MI was often significantly non-zero by statistical tests including a permutation test controlling for regional contiguity and hemispheric symmetry (P_{spin}; Fig. S5). For example, the left somatosensory cortex had strongly positive MI, indicating that the edges with strongest FC at baseline showed the greatest positive increase in FC during adolescence. Conversely, left posterior cingulate cortex had strongly negative MI, indicating that the edges with weakest FC at baseline showed the greatest positive increase in FC during adolescence (Fig. 2B). To put it another way, in somatosensory cortex and other regions with MI > 0 there was a conservative mode of developmental change: connections that were already strong at 14 become stronger by the age of 26. Whereas, in posterior cingulate cortex and other regions with MI < 0, there was a disruptive mode of developmental change: connections that were weak at 14 got stronger by the age of 26 (and connections that were strong at baseline became weaker) (Fig. 2C,D).

Conservative changes in connectivity were concentrated in primary motor and sensory areas, corresponding to cytoarchitectonic classes 1 and 5 in the von Economo atlas (24), and the insula (Fig. 3A). This anatomical distribution maps onto motor, ventral attention and visual networks previously defined by independent component analysis of adult resting state fMRI data (Fig. 3B) (25). Disruptive changes in connectivity were concentrated in association cortex (von Economo class 2) and limbic cortex, corresponding to fronto-parietal, default mode and limbic resting state networks. Subcortical nodes were almost all characterized by disruptive development, with weak baseline connectivity to association cortex becoming stronger, and strong baseline connectivity to primary motor or sensory cortex becoming weaker (Fig. 2D).

For further details on adolescent changes in functional connectivity at the finer grained level of edges, see SI Appendix, Fig. S6-S8.

Contextualising adolescent change in functional connectivity. We used a meta-analytic tool (Neurosynth; 26) to identify cognitive processes or experimental task conditions that were associated with prior task-related activation of disruptively vs. conservatively developing cortical systems (Fig. 3C,D). Disruptive changes in FC were located in cortical areas that were activated by memory, mentalising and social processing tasks. Conversely, conservative changes in FC were located in cortical areas that were activated by motor and sensory tasks.

We estimated cortical thickness shrinkage at each cortical node in a cross-sectional dataset of structural MRI scans collected from 297 of the participants in this fMRI study (1). The cortical areas with the most negative rates of thickness change (or fastest shrinkage) had the most negative MI ($\rho = 0.16$, $P = 0.0052$, $P_{\mathrm{spin}} = 0.036$; Fig. 4A). However, two other structural MRI markers of adolescent brain development were not significantly co-located with MI in this sample (SI Appendix, Fig. S9).

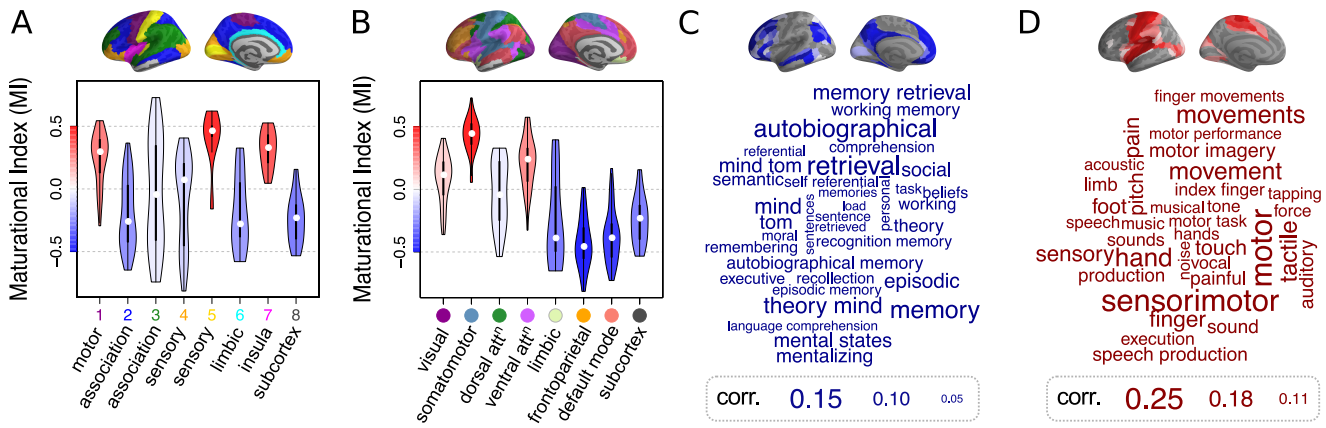

Fig. 3. Maturational index in anatomical and psychological context. A) Distribution of maturational index for each cytoarchitectonic class of the von Economo atlas (24), and B) for resting state networks derived from prior resting state FC analysis by Yeo (25). In both cases, subcortical regions were considered as an additional eighth class/subnetwork. The violin plots are coloured by average MI within the corresponding class of regions. C-D) Word clouds of cognitive terms associated with cortical brain regions that have C) disruptive (blue) or D) conservative (red) modes of development (Neurosynth decoding (26)). The size of cognitive terms corresponds to the correlation of corresponding meta-analytic maps generated by Neurosynth with each of the two modes (top).

We further compared the maturational index map (Fig. 2C) to nine independently produced maps of a range of brain functional and developmental parameters, including: (i) evolutionary and post-natal surface expansion of the cortex (27); (ii) metabolic rates of glucose, oxygen and aerobic glycolysis (AG) measured by PET (28); (iii) microarray measures of gene expression for 116 genes previously associated with AG (14) and extracted from the Allen Human Brain Atlas (29) as in (30); and (iv) areal scaling of the cortical surface (31).

We found that disruptive cortical regions (with negative MI) had faster rates of postnatal surface expansion (ρ = -0.28, $P = 8.7{\cdot}10^{-7}$, $P_{\text{spin}} = 0.036$), higher metabolic rates of glucose (ρ = -0.41, $P < 10^{-10}$, $P_{\text{spin}} = 0.0032$), higher rates of AG as measured by the glycolytic index (ρ = -0.56, $P < 10^{-10}$, $P_{\text{spin}} < 10^{-4}$), and higher expression of AG-related genes (ρ = -0.34, $P = 1.8{\cdot}10^{-5}$, $P_{\text{spin}} = 0.0006$) (Fig. 4B-D).

All P-values reported above were corrected for a total of 12 multiple comparisons using the false discovery rate (FDR). For details see Fig. 4 and SI Appendix Fig. S9 and Table S4.

Sensitivity analyses. To evaluate the robustness of our results, we verified that the MI is consistent when edge-wise FC_{14} and ΔFC_{14-26} are derived from 1,000 sets of independent random half-splits of the data (2x 260 scans), and when MI components are separately derived using cortico-cortical and subcortico-subcortical edges only (to account for potential differences in sub/cortical tSNR) (Fig. S10-S11).

Further, we repeated main analyses (Figs. 1-4) under five conditions: (i) using a different cortical parcellation (SI Appendix, Fig. S12-S15); (ii) in a subset of 298 cross-sectional scans (to rule out longitudinal effects of "regression to the mean"; SI Appendix, Fig. S16-S19); (iii) in a subset of 396 scans from a single scanner (to rule out scanner site effects; SI Appendix, Fig. S20-S23); (iv) in a subset of low-motion time-series from 182 scans, displaying no discernible motion (SI Appendix, Fig. S24-S28); and (v) in the whole sample preprocessed using global signal regression (GSR; SI Appendix, Fig. S29-S35). In all cases, the following key results of the main analysis were recapitulated: (i) two modes of adolescent change in functional connectivity were defined by positive and negative MI; (ii) conservatively maturing brain systems, defined by MI > 0, were concentrated in primary cortical areas, and disruptively maturing brain systems, defined by MI < 0, were concentrated in subcortical and association cortical areas; and (iii) disruptively maturing systems were significantly co-located with prior maps of aerobic glycolysis (AG) and AG-related gene expression. Additionally, FC_{14}, ΔFC_{14-26} and MI metrics were positively correlated between the main analysis and the sensitivity analyses of GSR pre-processed data, and a low-motion subset of data (SI Appendix, Fig. S36-37).

Discussion

We have reported results from an accelerated longitudinal study of adolescent development of functional connectivity (FC) in the healthy human brain. In a large, population-representative sample of resting-state fMRI data, balanced for age and sex, and controlled for head motion, we found evidence for two modes of maturational change in the age range 14 to 26 years, which we called conservative and disruptive.

The conservative mode of change was consolidating, or making stronger over the course of adolescence, the connectivity of specialised sensory or motor cortical areas that were already highly connected at age 14. Conservatively, "the rich get richer". In contrast, the disruptive mode of change was to make connectivity stronger in areas where it was relatively weak at age 14, or to make it weaker where it was relatively strong at the start of adolescence. Disruptively, "the rich get poorer and the poor get richer". Disruptive maturation was characteristic of association and limbic cortex, corresponding to default mode, fronto-parietal and limbic fMRI networks, and previously activated by tasks related to memory, theory of mind, and social cognition. Disruptive maturation was also characteristic of subcortical structures.

We hypothesised that the disruptive pattern of changes in macroscopic functional connectivity, measured by fMRI, was reflective of changes in microscopic, synaptic connectivity in association cortical and subcortical brain systems (2). We explored this hypothesis by comparing the fMRI map of maturational index (MI) to prior brain maps of structural, genomic and metabolic parameters of adolescent development.

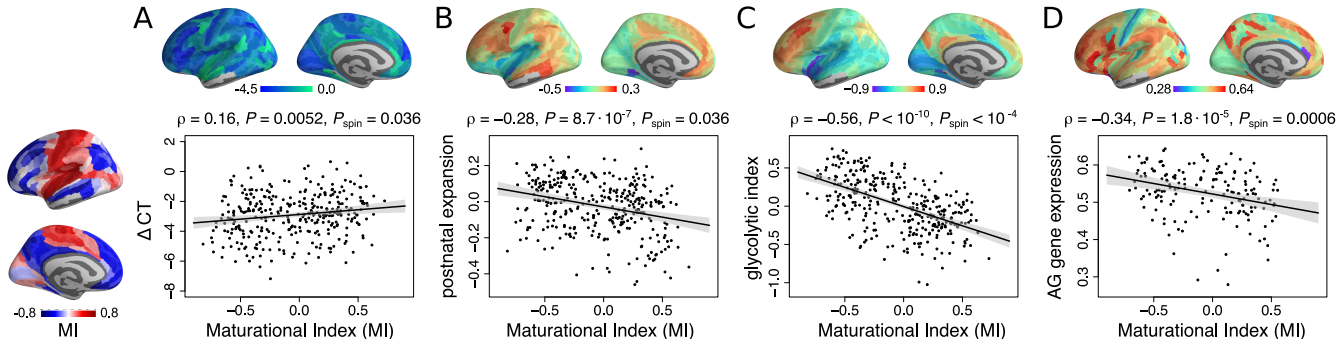

Fig. 4. Disruptive and conservative modes of fMRI maturation in developmental and metabolic context. A) Maturational index was positively correlated with ΔCT (1) - regions which had disruptive development (MI < 0) had faster rates of cortical thickness (CT) shrinkage during adolescence. B) MI was negatively correlated with a prior map of postnatal cortical surface area (28) - disruptive maturation was greater in regions that showed greatest expansion after birth. C) MI was negatively correlated with a prior map of the glycolytic index, a measure of aerobic glycolysis (AG; 28); and D) MI was negatively correlated with a prior map of brain regional expression of AG-related genes (29, 30).

Positron emission tomography (PET) has been used to map oxidative metabolism of glucose and non-oxidative metabolism of glucose in the presence of oxygen: aerobic glycolysis (AG). AG is thought to generate energy specifically for brain developmental processes and PET measurements of glycolytic index (GI) demonstrated that association cortex has sustained AG throughout adolescence to early adulthood (14, 28) (whereas primary cortical areas had relatively low AG after late childhood (14, 28)). We found that glycolytic index (GI) was highly correlated with maturational index (MI). Association cortical and subcortical regions with MI < 0 had GI > 0; whereas motor and sensory cortical areas with MI > 0 had GI < 0. This result was corroborated by the significant spatial correlation between a prior map of expression of AG-related genes and the fMRI map of MI. Disruptively developing brain regions had higher levels of AG-related genes than conservatively developing regions. We regard these convergent results as indicating that disruptive adolescent development of fMRI connectivity represents a metabolically expensive process of re-modelling in association cortex and subcortical structures.

We also found significant correspondence between the fMRI map of MI and the map of cortical shrinkage derived from structural MRI data in the same sample. Cortical shrinkage is the most well-replicated result in MRI studies of adolescent brain development and has been mechanistically explained as a marker of synaptic pruning and/or intra-cortical myelination (1). Another structural measure of developmental activity was provided by a prior map of post-natal expansion of cortical surface area (27). Association cortex has both greater surface area expansion and more disruptive development of FC. We regard these results as convergently indicating that disruption of FC between regions is co-located with cortical systems that are most structurally active in their adolescent development.

Finally, we used meta-analysis of existing task-related fMRI data to identify cognitive processes that activated cortical areas coinciding with the two modes of adolescent brain development. Conservative systems were activated by sensory and motor functions that would normally have been operational since early childhood. Disruptive systems were activated by a range of "higher-order" functions, such as working memory, theory-of-mind and autobiographical memory, which are later maturing social and cognitive processes.

These results generate the hypothesis that disruptive functional connectivity drives the emergence of more sophisticated socialising, mentalizing and executive skills as young people grow into independent adults. Moreover, they support the corollary hypothesis that psychiatric disorders or subclinical psychopathology could arise in young people from atypical maturation of association cortico-subcortical circuits (32–34).

Methodological issues. Strengths of the study include the accelerated longitudinal design and the balanced sample of healthy young people stratified by age and sex. Limitations include co-location of adolescent fMRI maps with prior maps of gene expression measured post mortem in adults, lack of simultaneously measured cognitive or behavioural data, and insufficient resolution of 3T MRI to measure the multiple functionally specialised sub-nuclei comprising subcortical nodes.

Concerning the crucial factor of in-scanner head motion (15–17): for our main analysis, we processed multi-echo (ME) fMRI time series with ME-ICA in an effort to disambiguate BOLD components from non-neuronal sources of fMRI dynamics (19, 20). This denoising step alone was not sufficient (23) so we used regression to further correct functional connectivity for linear dependence on head motion (FD regression) (21, 22). Data pre-processed by this pipeline passed standard QC criteria for head movement impact on functional connectivity (SI Appendix, Fig. S2). To assess the robustness of our results to this choice of movement correction pipeline, we conducted two major sensitivity analyses, of a low-motion dataset and of the whole dataset after motion correction by global signal regression (GSR). The results were not identical across main, low-motion and GSR analyses; but there are many possible factors, besides uncorrected or corrected effects of head motion, that could contribute to observed differences, e.g., the smaller sample size and shorter length of fMRI time series available for the low-motion analysis. However, it is reassuring that estimates of MI, baseline FC and adolescent change in FC were strongly correlated between different movement correction pipelines (SI Appendix, Fig. S36 and S37); and on this basis key results of our main analysis were replicated in the low-motion subset of scans and in the GSR-corrected scans; see SI Appendix for details.

Conclusion. Disruptive change in functional connectivity between association cortex and subcortical nuclei is likely reflective of a metabolically expensive process of human brain development in adolescence.

Materials and Methods

Participants. A demographically balanced cohort of 298 healthy adolescents (151 females) aged 14-26 years, scanned a total of 520 times, was included in this study. There were approximately equal numbers of male and female participants (∼60) in each of 5 age-defined strata at baseline: 14-15 years inclusive, 16-17 years, 18-19 years, 20-21 years and 22-24 years. The study was approved by the National Research Ethics Service, and conducted in accordance with NHS research governance standards. Participants aged 16 or older gave informed consent; younger participants gave informed assent and parental consent.

MRI acquisition and pre-processing. Scanning was at three sites, all operating identical 3T MRI systems (Magnetom TIM Trio, Siemens Healthcare, VB17 software). Resting-state fMRI data were acquired using a multi-echo EPI sequence (18): 263 volumes; TR = 2.42 s; GRAPPA with acceleration = 2; matrix size = 64 x 64 x 34; FOV = 240 x 240 mm; in-plane resolution = 3.75 x 3.75 mm; slice thickness = 3.75 mm with 10% gap, 34 oblique slices; bandwidth = 2368 Hz/pixel; TE = 13, 30.55, 48.1 ms.

For fMRI pre-processing, we used multi-echo independent component analysis (ME-ICA; 19, 20) to identify neuronal sources of fMRI variance that were retained to generate a time series at each voxel (35) which was bandpass filtered by the discrete wavelet transform (Daubechies 4 wavelet) to the frequency range 0.025-0.111 Hz. Geometric re-alignment of scan volumes was used to estimate 6 motion parameters (3 translation, 3 rotation), from which we derived estimates of volume-to-volume head motion - or framewise displacement (FD; 15). Mean FD was used as a measure of head movement in each scan session.

Parcellation and functional connectivity estimation. fMRI data were parcellated by a prior cortical template into 360 bilaterally symmetric regions (36), as well as 16 subcortical regions from FreeSurfer software (37), yielding a total of 376 regions. Regional fMRI time series were estimated by averaging over all voxels in each parcel. 30 cortical regions (near frontal and temporal poles) were excluded due to low regional mean signal, defined by a low Z-score of mean signal intensity ($Z < -1.96$) in at least one scan. For sensitivity analyses we used an alternative parcellation of cortex into 308 parcels of approximately equal surface area (∼5cm^2; 38, 39; see SI Appendix).

Functional connectivity (FC) matrices were estimated for each scan using Pearson's correlations between all pairs of regional time series. Age-related change in FC was modelled using linear mixed effect models that included age as the main fixed effect of interest, sex and scanner-site as fixed effect covariates, and a subject-specific intercept as a random effect (see SI Appendix for further details).

Data and code. Data has been uploaded to the Cambridge Data Repository: *[link inserted at proof stage]*. Code used to conduct analyses is available from FV's github: *[link inserted at proof stage]*.

ACKNOWLEDGMENTS. This study was supported by the Neuroscience in Psychiatry Network, a strategic award by the Wellcome Trust (095844/Z/11/Z) to the University of Cambridge and University College London. Additional support was provided by the National Institute for Health Research (NIHR) Cambridge Biomedical Research Centre. FV was supported by the Gates Cambridge Trust. PEV was supported by the MRC (MR/K020706/1) and is a Fellow of MQ: Transforming Mental Health (MQF17/24); PEV and KJW are Fellows of the Alan Turing Institute funded by EPSRC (EP/N510129/1). PF is a NIHR Senior Investigator (NF-SI-0514-10157), and was in part supported by the NIHR Collaboration for Leadership in Applied Health Research and Care (CLAHRC) North Thames at Barts Health NHS Trust. ETB is a NIHR Senior Investigator. The views expressed are those of the authors and not necessarily those of the NHS, the NIHR or the Department of Health and Social Care. The authors are grateful to Lena Dorfschmidt for corrections of analysis code.

1. Whitaker KJ, et al. (2016) Adolescence is associated with transcriptionally patterned consolidation of the hubs of the human brain connectome. *Proc. Natl. Acad. Sci. U. S. A.* 113(32):9105–9110.
2. Váša F, et al. (2018) Adolescent Tuning of Association Cortex in Human Structural Brain Networks. *Cereb. Cortex* 28(1):281–294.
3. Vertes PE, Bullmore ET (2015) Annual research review: Growth connectomics - the organization and reorganization of brain networks during normal and abnormal development. *Journal of Child Psychology and Psychiatry* 56(3):299–320.
4. Stevens MC (2016) The contributions of resting state and task-based functional connectivity studies to our understanding of adolescent brain network maturation. *Neurosci. Biobehav. Rev.* 70:13–32.
5. Paus T, Keshavan M, N. GJ (2008) Why do many psychiatric disorders emerge during adolescence? *Nat Rev Neurosci.* 9(12):947–957.
6. Bullmore E, Sporns O (2009) Complex brain networks: graph theoretical analysis of structural and functional systems. *Nat. Rev. Neurosci.* 10(3):186–198.
7. Fornito A, Zalesky A, Bullmore ET (2016) *Fundamentals of brain network analysis.* (Academic Press), 1st edition, p. 476.
8. Fair D, et al. (2007) Development of distinct control networks through segregation and integration. *Proc. Natl. Acad. Sci. U. S. A.* 104(33):13507–12.
9. Fair D, et al. (2009) Functional brain networks develop from a "local to distributed" organization. *PLoS Comput. Biol.* 5(5):e1000381.
10. Supekar K, Musen M, Menon V (2009) Development of large-scale functional brain networks in children. *PLoS Biol.* 7(7):e1000157.
11. Dosenbach NUF, et al. (2010) Prediction of individual brain maturity using fMRI. *Science* 329(5997):1358–1361.
12. Mills KL, Goddings AL, Clasen LS, Giedd JN, Blakemore SJ (2014) The developmental mismatch in structural brain maturation during adolescence. *Dev. Neurosci.* 36(3-4):147–60.
13. Marek S, Hwang K, Foran W, Hallquist MN, Luna B (2015) The Contribution of Network Organization and Integration to the Development of Cognitive Control. *PLoS Biol.* 13(12).
14. Goyal MS, Hawrylycz M, Miller JA, Snyder AZ, Raichle ME (2014) Aerobic glycolysis in the human brain is associated with development and neotenous gene expression. *Cell Matab* 19(2):49–57.
15. Power JD, Barnes KA, Snyder AZ, Schlaggar BL, Petersen SE (2012) Spurious but systematic correlations in functional connectivity MRI networks arise from subject motion. *Neuroimage* 59(3):2142–2154.
16. Satterthwaite TD, et al. (2012) Impact of in-scanner head motion on multiple measures of functional connectivity: Relevance for studies of neurodevelopment in youth. *Neuroimage* 60(1):623–632.
17. Satterthwaite TD, et al. (2013) Heterogeneous impact of motion on fundamental patterns of developmental changes in functional connectivity during youth. *Neuroimage* 83:45–57.
18. Barth M, Reichenbach JR, Venkatesan R, Moser E, Haacke EM (1999) High-resolution, multiple gradient-echo functional MRI at 1.5 T. *Magn. Reson. Imaging* 17(3):321–329.
19. Kundu P, Inati SJ, Evans JW, Luh WM, Bandettini Pa (2012) Differentiating BOLD and non-BOLD signals in fMRI time series using multi-echo EPI. *Neuroimage* 60(3):1759–70.
20. Kundu P, et al. (2013) Integrated strategy for improving functional connectivity mapping using multiecho fMRI. *Proc. Natl. Acad. Sci. U. S. A.* 110(40):16187–92.
21. Gu S, et al. (2015) Emergence of system roles in normative neurodevelopment. *Proc. Natl. Acad. Sci. U. S. A.* 112(44):13681–13686.
22. Satterthwaite TD, et al. (2019) Motion artifact in studies of functional connectivity: Characteristics and mitigation strategies. *Hum. Brain Mapp.* 40(7):2033–2051.
23. Power JD, et al. (2018) Ridding fMRI data of motion-related influences: Removal of signals with distinct spatial and physical bases in multiecho data. *Proc. Natl. Acad. Sci. U. S. A.* 115(9):E2105–E2114.
24. Vértes P, et al. (2016) Gene transcription profiles associated with inter-modular hubs and connection distance in human functional magnetic resonance imaging networks. *Philos. Trans. R. Soc. B Biol. Sci.* 371(1705).
25. Yeo BTT, et al. (2011) The organization of the human cerebral cortex estimated by intrinsic functional connectivity. *J. Neurophysiol.* 106(3).
26. Yarkoni T, Poldrack RA, Nichols TE, Van Essen DC, Wager TD (2011) Large-scale automated synthesis of human functional neuroimaging data. *Nat. Methods* 8(8):665–670.
27. Hill J, et al. (2010) Similar patterns of cortical expansion during human development and evolution. *Proc. Natl. Acad. Sci. U. S. A.* 107(29):13135–40.
28. Vaishnavi SN, et al. (2010) Regional aerobic glycolysis in the human brain. *Proc. Natl. Acad. Sci. U. S. A.* 107(41):17757–17762.
29. Hawrylycz MJ, Lein ES, Guillozet-Bongaarts AL, Shen EH, Ng Lea (2012) An anatomically comprehensive atlas of the adult human brain transcriptome. *Nature* 489(7416):391–399.
30. Arnatkeviciute A, Fulcher BD, Fornito A (2019) A practical guide to linking brain-wide gene expression and neuroimaging data. *Neuroimage* 189(July 2018):353–367.
31. Reardon PK, et al. (2018) Normative brain size variation and brain shape diversity in humans. *Science* 360(6394):1222–1227.
32. Heller AS (2016) Cortical-subcortical interactions in depression: From animal models to human psychopathology. *Front Syst Neurosci* 10(20).
33. Wise T, et al. (2017) Instability of default mode network connectivity in major depression: a two-sample confirmation study. *Transl Psychiatry* 7(4):e1105.
34. Ziegler G, et al. (2019) Compulsivity and impulsivity traits linked to attenuated developmental frontostriatal myelination trajectories. *Nature Neuroscience* 22:992—999.
35. Posse S, et al. (1999) Enhancement of BOLD-contrast sensitivity by single-shot multi-echo functional MR imaging. *Magn. Reson. Med.* 42(1):87–97.
36. Glasser MF, et al. (2016) A multi-modal parcellation of human cerebral cortex. *Nature.*
37. Filipek PA, Richelme C, Kennedy DN, Caviness VS (1994) The Young Adult Human Brain: An MRI-based Morphometric Analysis. *Cereb. Cortex* 4(4):344–360.
38. Desikan RS, et al. (2006) An automated labeling system for subdividing the human cerebral cortex on MRI scans into gyral based regions of interest. *Neuroimage* 31(3):968–980.
39. Romero-Garcia R, Atienza M, Clemmensen LH, Cantero JL (2012) Effects of network resolution on topological properties of human neocortex. *Neuroimage* 59(4):3522–3532.